Mathematical Human Body Models in Side Impacts – A Validation Study with Particular Emphasis on the Torso and Shoulder and their Influence on Head and Neck Motion

Bengt Pipkorn*, Peter Halldin**, Lotta Jakobsson***, Johan Iraeus****, Maria Backlund***, Krystoffer Mroz*, Daniel Lanner**, Kristian Holmqvist*****, Svein Kleiven**

*Autoliv Research, **KTH, ***Volvo Cars, ****Epsilon and *****Chalmers University of Technology

ABSTRACT

The ability of three mathematical human body models to predict previously published human responses in two different side impact loading configurations was evaluated using an objective rating method. In particular the kinematics of the shoulder, T1 and head were evaluated. The human body models evaluated were THUMS, HUMOS 2 and the GM model. The impact loading configurations used were pendulum impact tests and sled tests.

In the pendulum configurations, the closest correlation to the published responses was shown by THUMS followed by the GM model. In the sled configuration, closest correlation to the published responses was shown by HUMOS 2 followed by THUMS.

According to the objective rating method the published responses in the pendulum configuration were predicted by all human body models. The published responses in the sled configuration were predicted by HUMOS 2 and THUMS.

Keywords: Human Body Models, THUMS, HUMOS, Side Impact, Pendulum, Sled

SIDE IMPACTS ARE the second most frequent type of crashes causing serious injury and death to occupants in cars (Acierno et al., 2003). In terms of AIS2+ injury outcomes in modern cars, head (28% of AIS2+ injuries to front seat occupants) and chest injuries (22%) still dominate although injuries to the abdomen (10%), upper extremity (14%) and lower extremity (including pelvis) are also observed (Welsh, 2007). When only AIS4+ injuries are considered, head (36%), chest (41%) and abdomen injuries (31%) comprise the overwhelming majority of injuries.

In a side impact the head impact location and impact velocity are in the early phase influenced by the load transfer from the upper spine. The upper spine is influenced by the primary impact to the shoulder and chest wall and its interaction with the ribcage, spine and the thoracic organs. Hence these load paths control the location and the velocity of the head impact in a side impact.

The mathematical human body models are developed with the intention to improve our understanding of the structural consequences in the human body of blunt trauma and to predict injury risks. The models enable the calculation of physical variables mechanically related to injury, e.g. plastic strain (Rouhana et al., 2003). In addition the models can be used to assess complex mechanics that can not be assessed using mechanical anthropomorfic tests devices (ATDs) with single-point sliders etc, and limitations of macro-level injury criteria (Kent et al., 2001; Cesari et al., 1994; Rouhana et al., 2003; Peitjean et al., 2002).

Mathematical finite element models of the fiftieth percentile "average" male have been of primary interest and several have been developed. Such models are the THUMS (The Total Human Model for Safety) model, the MADYMO human model, the Human Model for safety version 2 (HUMOS 2), the General Motors (GM) human body model and the H-model etc. Details about the various models have been presented by Yang et al. (2006). The models have complex humanlike representation of the spine. The individual vertebras and inter vertebral discs are all represented. However, the models have not been evaluated for neck induced head motion caused by side loading to the shoulder and chest of the occupant.

The aim of this study was to evaluate the ability of the human body models THUMS, HUMOS 2 and GM model to predict PMHS kinematics and responses in side impact loading. Of particular interest was to evaluate the ability to predict upper body, head and neck kinematics.

METHODOLOGY

In the evaluation of the human body models the predictions were compared to results from available publications of mechanical tests with post mortem human subjects (PMHS). In the evaluation of the mechanical test results particular emphasis was placed on the upper body kinematics of the occupant. When available also head and neck kinematics were evaluated. The models were evaluated by means of both pendulum impact tests and sled tests. The test configurations were:

1. Lateral padded pendulum impact tests at 3.95 – 4.51 m/s, (Bolte 2004).
2. Lateral unpadded sled tests at 6.7 m/s (Cavanaugh et al., 1990, 1993 and 1996).

In the lateral pendulum impact tests three PMHS were used. The PMHS were seated in an upright position on a Teflon coated test seat. The arms were symmetrically resting in the knee of the subjects. A pendulum with a padded surface and a mass of 22.9 kg was impacting the PMHS. The shape of the pendulum head was rectangular with the dimensions 150 x 80 mm. The padding was 50 mm thick Arcel 310. The centre was aligned with the palpated glenohumeral joint in the x-direction (Figure 1). In the z-direction the height of the subject was positioned in such a way that the centre of the pendulum impacted the PMHS 50 mm below the glenohumeral joint. In the mechanical tests the impact velocity varied between 3.95 and 4.51 m/s. The velocity was chosen at such a low level to avoid injuries to the shoulder girdle. Each PMHS was impacted once pure laterally.

In the pendulum experiments 11 accelerometers were used. One accelerometer was mounted on the impactor. On the PMHS ten tri-axial accelerometers were mounted on eight anatomical regions. These regions were: left acromion, right acromion, manubrium sterni and the spinous process of the first thoracic vertebra (T1), left scapulae, right scapulae, left collar bone, right collar bone. On left and right collar bone 2 accelerometers were mounted. The data from each accelerometer was transformed to initially coincide with the global coordinate system. The PMHS were equipped with photo-targets at the same locations as the accelerometers. The films were obtained and digitized using TEMA 3D (TEMA 3D). The global head movement was measured by digitizing the contour of the head.

In the mathematical pendulum impact configuration model the impactor velocity was 4.34 m/s. The measurements used for evaluation was acceleration of the impactor and relative y-displacement between:

       Pendulum vs left acromion
       Pendulum vs right acromion
       Pendulum vs T1
       Pendulum vs sternum.

In addition the head x-rotation and z-displacement was the evaluated.

In the pendulum impact tests and in the sled tests the defined local coordinate system was the x-axis directed forward, the y-axis to the left and the z-axis pointing upwards (Figure 1).
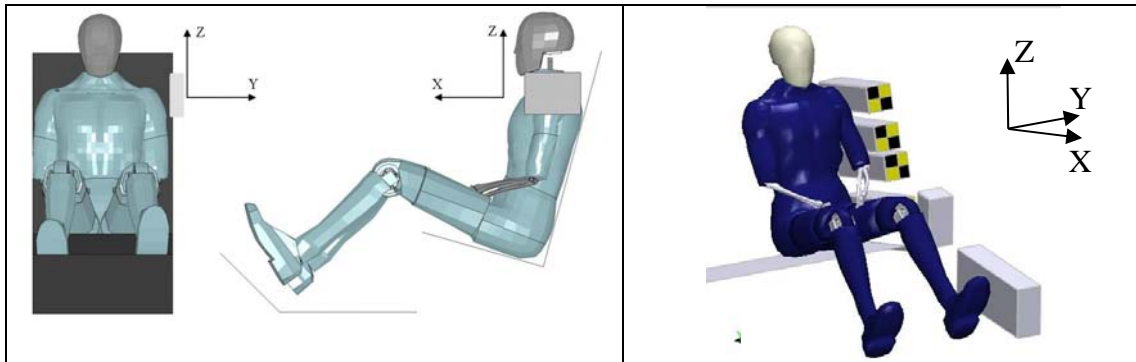

Figure 1. Definition of Coordinate System in the Pendulum and Sled Configurations

In the Wayne State sled tests a Heidelberg type seat structure was used. The PMHS was seated on a Teflon coated sheet and the back was supported by two rods. The sled together with the PMHS was accelerated to a constant speed on a 40 m long track. At the end of the track the sled was decelerated to rest by means of a hydraulic damper and the PMHS continued sliding until laterally impacting the fixed wall. The impacted wall was vertically divided into four sections. The uppermost section impacted the shoulder area, the next from the top the thorax area, the second from below the abdominal area and the lowest the pelvic area. A fifth impacting area was located at the knee. All these impact areas were equipped with force transducers. In the tests the sled and PMHS were accelerated to a velocity of 6.7 m/s and four PMHS were tested.

The PMHS were instrumented with tri-axial accelerometers at the head, first thoracic vertebra (T1), twelfth thoracic vertebrae (T12), sacrum and left and right acromion. Uni axial accelerometers were mounted at the upper and lower sternum and left and right rib four and eight. The PMHS were also equipped with photo-targets. On T1 and T12 the target was mounted on the spinous process of the vertebras. The films were obtained and the photo targets were digitized using TEMA 3D. The global head movement was also measured by manually digitizing the contour of the head.

In the sled tests the arms were positioned slightly anterior to the mid-auxiliary line by tying the arms together at the wrists with duct-tape and letting the arms rest on the lap (Cavanaugh et al., 1993).

The finite element human body models used for evaluation were the THUMS, HUMOS 2 and the GM model. The THUMS was developed by Toyota. The model consists of 87 000 elements. The ribs are modelled with one solid element through the thickness representing the trabecular bone covered by shell elements representing the cortical bone. The shoulder complex is represented by interior contacts between the humerus and scapula and the ligaments are represented by springs. A number of evaluations of the model have been carried out and reported (Oshita et al., 2002; Iwamoto et al., 2001; Iwamoto et al., 2003; Iwamoto et al., 2005 and Chawla et al., 2005).

The HUMOS 2 model used was developed within the EC funded program HUMOS (Robbin, 2001, Vezin and Verreist 2005). The model consists of about 80 000 elements. The ribs are modelled with three elements through the thickness of the rib representing the trabecular bone covered by shell elements representing the cortical bone. The material model used for the trabecular bone is elastic while the material model used for the trabecular bone is

elastoplastic. The shoulder complex is represented by interior contacts between the humerus and scapula and the ligaments are represented by springs. Within the EC program the model was validated mainly by means of frontal impact sled tests at 30 km/h up to 60 km/h.

The original GM model was developed by Deng et al., (1999a, 1999b). The model was further developed by Chang (2001) by adding extremities and the shoulder complex. Thereafter the model was updated by Lindquist et al., (2007). The update aimed at validating the model for upper body kinematics in frontal impact by adding muscles, Hybrid III head and lower extremities. The model consists of 63 000 elements. The ribs are modelled with eight elements through the thickness representing both the trabecular and cortical bone. The material model used is elastoplastic. The shoulder complex is represented by a spherical joint between humerus and scapula.

For the study the human body models were instrumented with accelerometers at the same anatomical locations as the PMHS in the published studies. In addition, an accelerometer measuring global movement was defined in the models to capture the head Centre of Gravity movement.

In modelling the pendulum impact tests the human body models were positioned on top of a rigid flat surface in an upright position. The friction coefficient was 0.1. The models were positioned as similar to the PMHS as possible with the arms resting on the lap. There was a small angle between the humerus and the back support and the elbow was positioned lateral to the head of the humerus. The pendulum was impacting the human body models 50 mm below the glenohumeral joint.

In modelling the sled test configuration the human FE models were initially positioned with the back against a plane representing the two rods in the mechanical test set-up. The human body models were positioned so that the uppermost part of the left clavicle was located 570 mm above the nominal seat plane for the unpadded tests. The arms were rotated 15 degrees forward from the mid-auxiliary line and resting in the lap.

To allow for a comparison between the published PMHS results and the predictions from the mathematical human body all PMHS acceleration measurements were scaled to a 50%-ile male using a scaling method proposed by Eppinger et al. (1984).

To assess the quality of the human body model predictions relative to the published mechanical PMHS test results and an objective rating method (ORM) was used (Hovenga et al., 2005). The method evaluates the correlation between two signals by scalar values, such as peak values and peak times (Figure 2). In addition the method evaluates curve shapes. A complete ORM value for each of the two load cases was also calculated based on the individual scalar and shape ORM values.
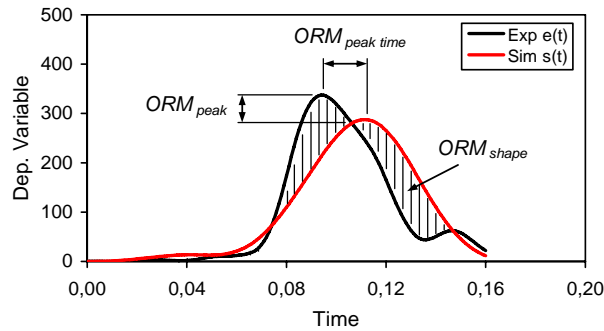
Figure 2: Objective Rating Method – ORM

In this study, the signals according to Table 1 were used for the ORM evaluation. The signals were grouped in pendulum tests and sled tests. The ORM scalar and shape comparisons were limited to the time frame of 0-60 ms, except for the head displacement comparisons in which a time frame of 0 - 120 ms was used.

Table 1: Signals Used for Evaluation

Config	Signal	Signal
Bolte Pendulum	Head Global X-Rotation Head Global Y-Displacement Head Global Y-Displacement Head Global Z-Displacement	Pendulum Relative Right Acromion Y-Displacement Pendulum Relative Left Acromion Y-Displacement Pendulum Relative T1 Y-Displacement Pendulum Y-Acceleration
Wayne State Sled	Head Global X-Rotation Head Global Y-Displacement Head Global Z-Displacement T1 Relative Head Y-Displacement T1 Relative Head Y-Displacement	Acromion Left Global Y-Displacement T1 Relative Left Acromion Y-Displacement T1 Relatvie Left Acromion Y-Velocity T1 Global Y-Displacement T12 Global Y-Displacement

The scalar ORM values were determined based on the Factor Method according to Equation 1. The resulting comparison between the experiment (exp) and the simulation (sim) range between 0 and 100%, where 100% corresponds to a perfect match.

$$ORM_{scalar} = \frac{\max(0, exp \cdot sim)}{\max(exp^2, sim^2)} \qquad (1)$$

The correlation of the curve shapes between the experiment (e(t)) and the simulation (s(t)) was determined based on equation 2 which is called the Weighted Integrated Factor Method. In this method, a scalar value is calculated according to Equation 1 for each point of the curve. Also, a weight factor, based on the maximum value of the experimental and simulation signal at each point, is applied. The sum of all points was then determined using the Root Mean Square Addition Method.

$$ORM_{shape} = 1 - \sqrt{\frac{\int \left(\max(|e(t)|, |s(t)|) \cdot \left(1 - \frac{\max(0, e(t) \cdot s(t))}{\max(e(t)^2, s(t)^2)} \right)^2 \right) dt}{\int \max(|e(t)|, |s(t)|) dt}}$$ (2)

The ORM value for the complete system was calculated according to equation 3, where the root mean square addition method was applied to all scalar values of the system. W was a weight factor for each scalar value. In this study the weight W=1.0 was applied to all scalar values.

$$ORM_{complete} = 1 - \sqrt{\frac{\sum W_{scalar\ or\ shape} \cdot (1 - ORM_{scalar\ or\ shape})^2}{\sum W_{scalar\ or\ shape}}}$$ (3)

If a peak value is not reached during the time frame the end time will be used in the peak time evaluation. That means if the end time is used a perfect match (100%) for the peak time evaluation will be obtained.

RESULTS

Results Pendulum Impact Validation

All pendulum impact result plots can be found in Appendix A. For the pendulum peak value evaluation the peak value scores varied from 45% - 99% (Figure 3). For the GM model the peak value score varied from 45% - 99% with a mean of 79%. For HUMOS 2 the peak value score varied from 57% - 98% with a mean of 80%. For THUMS the peak value score varied from 64% - 97% with a mean of 78%. Generally low head rotation and displacement peak value score was obtained with HUMOS 2. High head y-displacement score was obtained with THUMS and high pendulum relative right acromion y-displacement was obtained with the GM model.

The peak time scores varied from 66% - 100%. For the GM model the peak time score varied from 73% - 97% with a mean of 89%. For HUMOS 2 the peak time score varied from 66% - 100% with a mean of 87%. For THUMS the peak time score varied from 70% - 100% with a mean of 78%. In all configurations but one THUMS peak score was the lowest of the three models.
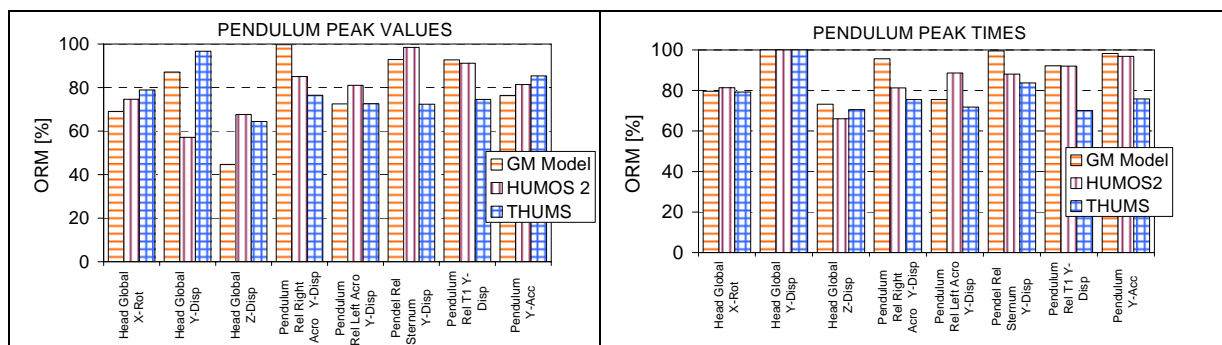

Figure 3. Pendulum Peak Value and Peak Time Evaluation

For the pendulum curve shape evaluation the score varied from 25% - 98% with a mean of 75% (Figure 4). For the GM model the curve shape score varied from 49% -97% with a mean of 80%. For HUMOS 2 the curve shape score varied from 25% - 87% with a mean of 70%. For THUMS the curve shape score varied from 64% - 88% with a mean of 75%. In all configurations but two, highest curve shape score was obtained with the GM model.
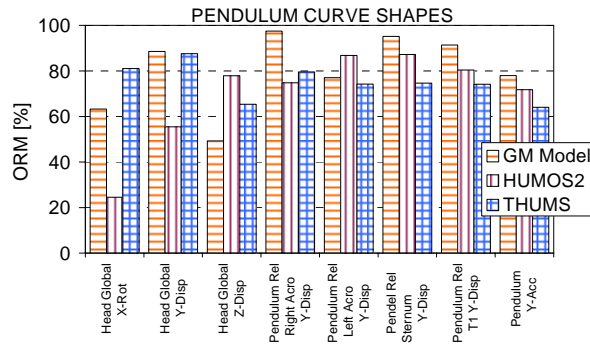
Figure 4 Pendulum Curve Shape Evaluation

Results Sled Test Validation

All sled test result plots can be found in Appendix B. For the sled peak value evaluation the peak value scores varied between 50% - 99% (Figure 5). For the GM model the peak value score varied between 50% - 95% with a mean of 72%. For HUMOS 2 peak value score varied between 69% - 96% with a mean of 85%. For THUMS the peak value score varied between 57% - 99% with a mean of 84%. Generally, a high head rotation and displacement score was obtained with all human body models. Low relative T1 peak value scores were obtained with the GM model.

For the peak time evaluation the scores varied between 19% - 100% (Figure 5). For the GM model the peak time score varied between 29% - 100% with a mean of 81%. For HUMOS 2 the peak time score varied between 19% - 100% with a mean of 84%. For THUMS the peak time score varied between 23% - 100% with a mean of 84%. For all models a low score was obtained for the left acromion y-displacement.
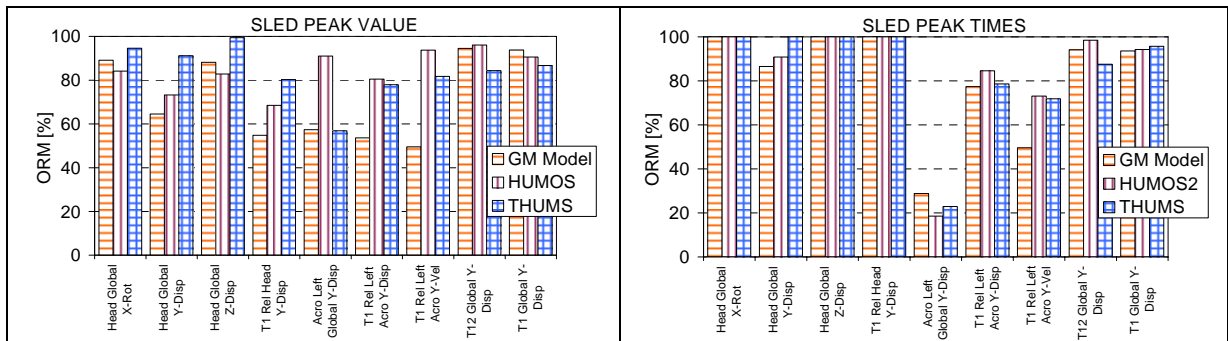

Figure 5 Wayne State Sled Peak Value and Peak Time Evaluation

For the curve shape evaluation in the sled test configuration curve shape score varied between 27% - 96% (Figure 6). For the GM model the curve shape score varied between 27% - 89% with a mean of 58%. For HUMOS 2 the curve shape score varied between 48% - 96% with a mean of 73%. For THUMS the curve shape score varied between 29% -94% with a mean of 70%. For all models a low score was obtained for the relative y-velocity between T1 and left acromion. Generally a high score was obtained for head rotation and head z-displacement.
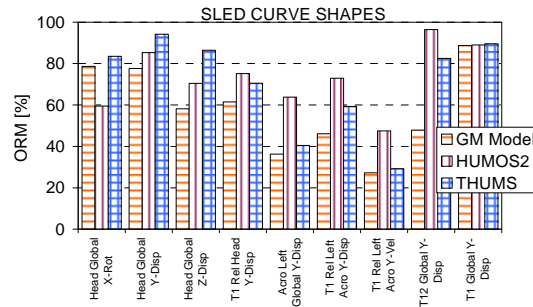
Figure 6. Wayne State Sled Curve Shape Evaluation

Results Complete Validation

For the complete validation the score in the pendulum configuration was 77% for the GM model, 73% for HUMOS 2 and 78% for THUMS (Figure 7). In the sled configuration the score was 63% for the GM model, 74% for HUMOS 2 and 71% for THUMS. The GM model and THUMS both had lower scores in the sled configuration than in the pendulum configuration. For HUMOS 2 the total score was higher in the sled configuration than in the pendulum configuration.
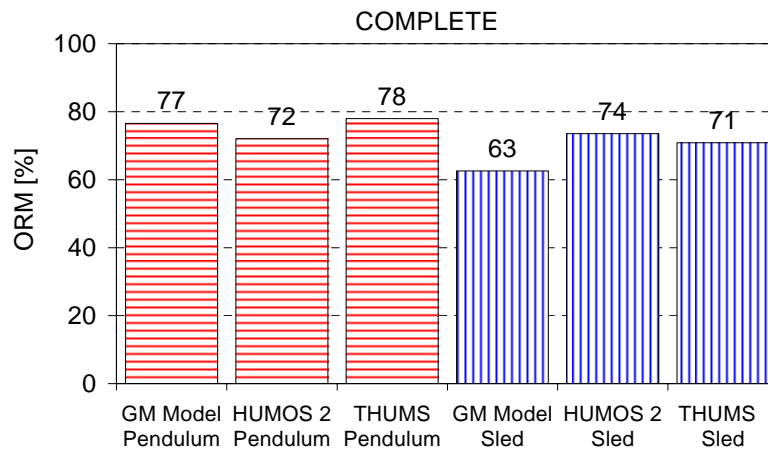

Figure 7. Complete Rating

DISCUSSION

The complete ORM rating score varied from 63% - 78%. Good correlation was in a study by Hovenga et al., (2005) defined to be an ORM score of 65% or higher. Therefore good correlation was obtained for the human body models in all configurations but one. The GM model in the sled configuration obtained an ORM score of 63% which was regarded as not good correlation.

In both the pendulum and sled analysis 60 ms was chosen as end time except for in the head analysis in the pendulum configuration. In the pendulum all upper body peak values were reached in 60ms. Peak values for the head occurred later therefore 100 ms was used for the head evaluation in the pendulum configuration. In the sled tests all peak values for the upper body were reached in 60 ms. The head impacted the sled at about 60 ms. Therefore in the sled analysis 60 ms was chosen as end time also for the head.

In the peak time analysis if the models have not reached a peak value the peak time will be calculated at the end of the analysis time. In particular in the sled peak time analysis a number of the signals reached 100% agreement indicating that a peak value was not reached for the analysis.

For the GM model there was a significantly lower ORM score for the sled configuration relative to the score in the pendulum configuration. In the sled configuration in addition to loading the upper body, the wall also loaded the pelvis and legs of the PMHS as published by Cavanaugh et al., (1990, 1993 and 1996). In the GM model the pelvis and the lower extremities were from a Hybrid III model. Therefore the reason for the poor ORM score of the GM model in the sled configuration can be due to fact that the pelvis and lower extremities of the model were not modelled as human.

In the published mechanical pendulum and sled tests some of the PMHS sustained injuries. In the lateral pendulum impacts tests there was only one PMHS that sustained an injury (Table 2). The injury was a loose sternoclavicular joint. It was assumed that the kinematics of the PMHS was not significantly influenced by the injury. Therefore the results from the tests were included in the evaluation.

Table 2. Summary of Injuries Received in Lateral Pendulum Impact Tests

Tests	Side	Joint Injury	Bone Injury
Lat01	Left	None	None
	Right	None	None
Lat02	Left	Loose Sternoclavicular joint	None
	Right	None	None
Lat04	Left	None	None
	Right	None	None

In the published unpadded sled tests at 6.7 m/s all PMHS sustained injuries (Table 3). The injuries were mainly fractures. It is likely that the chest kinematics of the PMHS was altered by the fractures. In the human body models there were failure criteria defined for the ribs. In the sled configuration for all human body models numerous ribs reached the failure criteria levels and the failed elements were eliminated. The elimination of elements resulted in reduced stiffness of the chests. Therefore the model responses can be considered valid to compare to the published sled test PMHS results. However, in future analysis the influence of bone fracture on occupant kinematics will be evaluated in more detail with the human body models.

Table 3. Summary of Injuries Sustained in Unpadded Sled Tests at 6.7 m/s

Tests	Shoulder Injury	Chest Injury
SIC05	None	12 Left Rib Fractures 8 Right Rib Fractures
SIC07	Left Acromioclavicular SeparationLeft Calvicle Fracture	13 Left Rib Fractures 3 Right Rib Fractures
SIC08	Left Acromioclavicular SeparationLeft Calvicle Fracure	15 Left Rib Fractures 9 Right Rib Fractures
SIC131	Left Clavicle Fracture	8 Left Rib Fracture

In the pure lateral pendulum impact test evaluation of the shoulder kinematics generally the relative displacements in x- and z-direction were less than 20% of the displacements in y-direction. Therefore in the evaluation of the human body models the y-displacements were evaluated.

Head and T1 kinematics was manually digitized. In the sled tests only one of the tests was recorded with a camera view that allowed for tracking of the head and T1. Therefore for the sled test evaluation head displacement and T1 displacement for only one of the published PMHS was used for model evaluation. There were no photo targets on the heads of the PMHS. Therefore the rotation and displacement of the head was digitized using the contour of

the head. The centre of the contour might not be the coincident with the centre of gravity of the head.

In the evaluation of head kinematics in the sled test configuration, the initial 15 ms of head - T1 relative rotation was captured by the GM and HUMOS 2 models (Appendix B). For THUMS there was less head - T1 relative rotation during the initial 15 ms. From 15 to 45 ms the head rotations of the GM model, HUMOS 2 and THUMS were smaller than for the PMHS (Figure 8). For THUMS the time offset between the model and the test was due to the delay of the shoulder upload in T1, which resulted in an offset of the displacement response. The reason for the difference for the GM model in the later phase can be the smaller head mass (3.5 kg) compared to the other two model masses (app. 4.4 kg). Also, a possibly too stiff neck can be present in the GM model. For the HUMOS 2 model, the vertical distance between T1 and the head centre was observed to be 161 mm. It is significantly less than for the other two models (THUMS 192 mm and GM model 196 mm). The short distance can also be a reason for the differences in head kinematics.
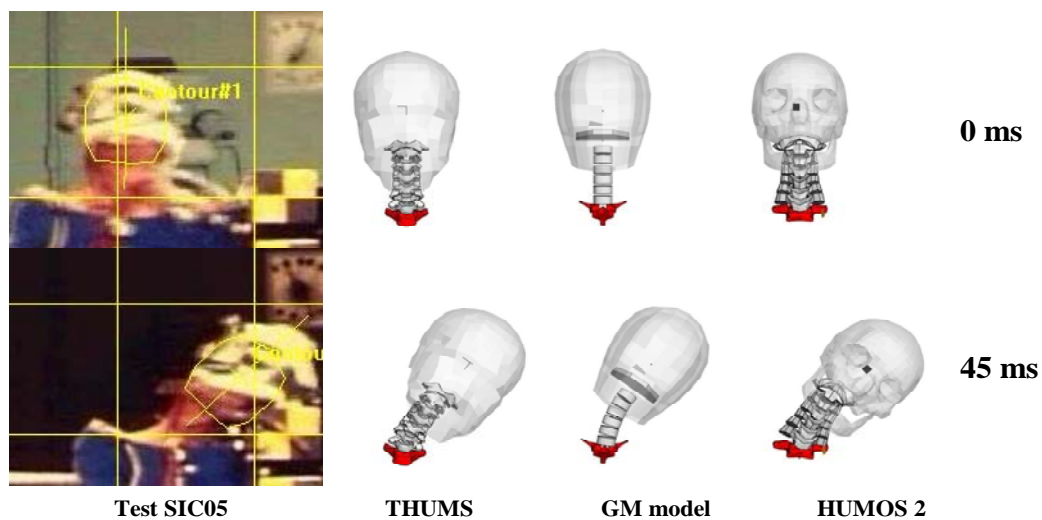

| Test SIC05 | THUMS | GM model | HUMOS 2 |

Figure 8. Head Kinematics of PMHS Subject SIC05 (Cavanaugh et al.), THUMS, the GM Model and HUMOS 2 in the Unpadded sled tests at 6.7 m/s (T1 Vertebra Marked in Red)

In the human body models there were some differences in the representation of, for the study important, anatomical parts. One such anatomical part was the shoulder complex. The model response in the pendulum configuration was significantly influenced by how the shoulder was modelled. Different modelling strategies were applied in the human body models to model the glenohumeral joint. In the GM model a spherical joint between humerus and scapula was used while the shoulder complex was modelled more human like in THUMS and HUMOS 2 (Figure **9**). In THUMS and HUMOS 2 the shoulder complex was represented by interior contacts between the humerus and the scapula and the ligaments were represented by springs. A relative displacement of the humerus relative to the scapula was therefore allowed. In the spherical joint only rotations were permitted. However, the spherical joint used in the GM model made the model robust. The joint also made the shoulder complex stiff. The shoulder model of HUMOS 2 was also very stiff despite the fact that the representation of the shoulder complex was more human-like.
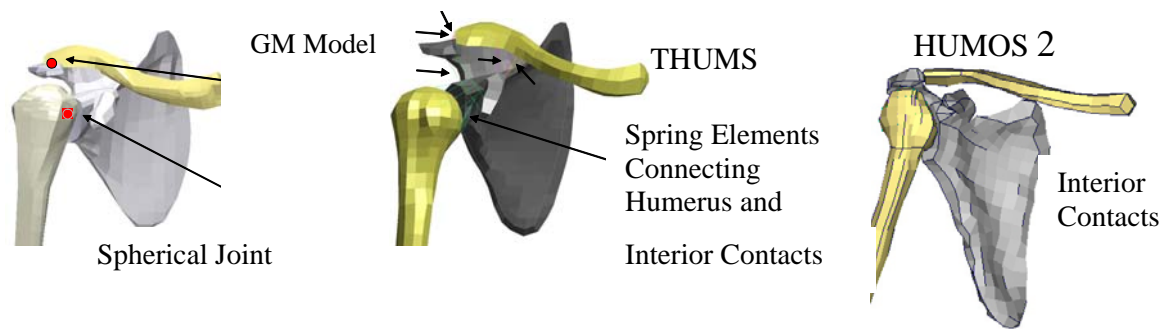
Figure 9. Shoulder Representation in the GM model, THUMS and HUMOS 2

Other important anatomical differences were the representation of the chest (Figure 10). The GM model and THUMS ribcage was barrel shaped while the HUMOS 2 was cone shaped. That means that in the GM model and THUMS the length of the ribs was increasing from rib one to seven and thereafter decreasing. For HUMOS 2 the length of the ribs was increasing from rib one to ten and thereafter decreasing. In HUMOS 2 there was a significant distance between the scapula and the ribcage. In addition the coverage of the scapula varied. Normally the scapula covers ribs two to seven (Tortora, 1996). In the GM model rib one was also covered by the scapula. For THUMS and HUMOS 2 rib eight was covered by the scapula. The inclination of the ribs also varied between the models. The least inclination was for HUMOS 2 and the greatest inclination was for THUMS. It has been shown in frontal loading of the chest that the inclination of the ribs influences the stiffness of the chest (Kent et al., 2005). In future analysis the influence of rib inclination on chest stiffness in side loading will be evaluated.
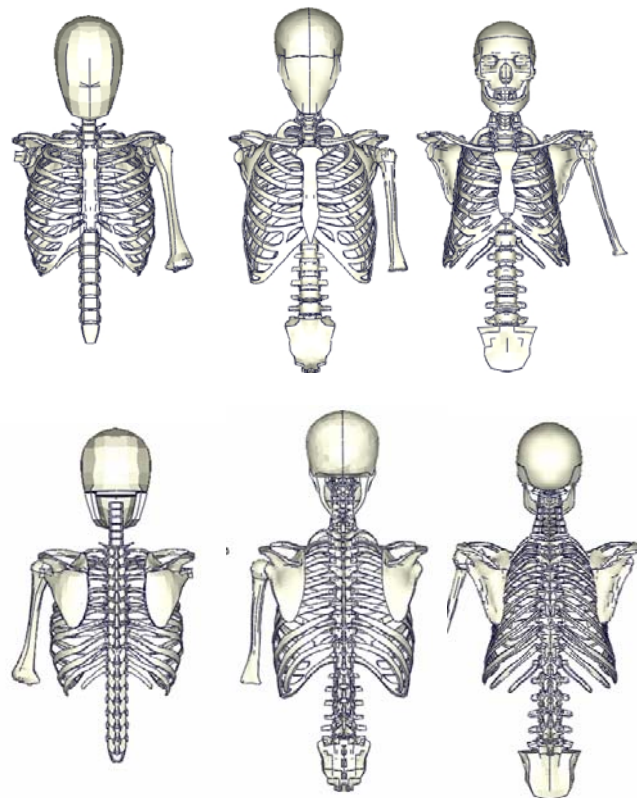

Figure 10. GM Model, THUMS and HUMOS 2 Anterior and Posterior View

In the GM model some ligaments connecting the scapula and the humerus were not included. Therefore in the sled tests the winging out of the scapula was pronounced.

In both the GM model and THUMS model there was a thick layer of arm flesh covering the humerus proximal head. Based on acromion accelerometer signals from the PMHS tests the distance the acromion travels before stopping was 18-35 mm with an average of 23 mm for all tests. This was consistent with the observations of Koh (2001) who concluded that the skeletal deflection (T1 to acromion) was about an inch (25 mm) less than the overall deformation (T1 to shoulder edge). The distance between acromion and the impactor at time zero was about 70 mm in the GM Model, 60 mm for the THUMS model and 35 mm for the HUMOS 2 model. This was 45 mm, 35 mm and 12 mm more than for the PMHS tests or with a velocity of 6.2 m/s, a time delay of 7 ms, 6 ms and 2 ms respectively. Repositioning the arm and decreasing the arm flesh thickness can improve the initial response in the acromion for the human body models.

The deformation pattern of the thorax was different between the FE models. One of the major differences in addition to the geometrical differences between the models was the modelling of the coastal cartilage. The modulus of elasticity used in the GM model was ten times as large as the one that was used in the THUMS model. Comparing the cartilage stiffness in the literature to the FE models the stiffness of THUMS was closer to the data found in the literature than the GM model. For the HUMOS 2 model the modulus of elasticity was 50 MPa, which was in-between the values for the other two models. Furthermore in THUMS a plasticity curve was defined that effectively limited the stress to below 10 MPa. In the GM model and the HUMOS 2 model a linear elastic material model was used. However, the modulus is usually measured in quasi static conditions but the material can be expected to be quite rate dependent, as many biological materials in fact are. The sled test predictions indicate that the modulus of elasticity of the PMHS is somewhere between the modulus used in the GM model and THUMS.

CONCLUSION
- All human body models predicted previously published PMHS responses in pendulum tests.
- All models but one predicted previously published PMHS responses in sled tests.
- Highest objective rating score in the pendulum configuration was obtained by THUMS
- Highest object rating score in the sled configuration was obtained by HUMOS 2
- Highest total objective rating score was obtained by THUMS
- Closest predictions of previously published PMHS head kinematics was shown by THUMS

REFERENCES
Acierno S., Kaufman R., Rivara F. P., Grossmann D. C., Mock, C., CIREN Seattle, Vehicle Mismatch Injury Patterns and Severity, 2003

Bolte JH. Injury and Impact Respons of the Shoulder due to Lateral and Oblique Loading. PhD. Dissertation paper, 2004

Cavanaugh J. M., Walilko T., Nalhotra A., Zhu Y., King A. I., Biomechanical Response and Injury Tolerance of the Thorax in Twelve Sled Side Impacts, Proc. 34th Stapp Car Crash Conf., SAE Paper No: 902307, SAE , Warrendale, Pennsylvania, 1990

Cavanaugh J. M., Zhu YJ, Huang Y, King A.I., Performance and Mechanical Properties of Various Padding Materials Used in Cadaveric Side Impact Sled Tests. SAE Paper No 920354, 1992

Cavanaugh J. M., Zhu Y., Huang Y., King A. I., Injury and Response of the Thorax in Side Impact Cadaveric Tests., Proc. 37th Stapp Car Crash Conf., SAE Paper No: 933127, SAE, Warrendale, Pennsylvania, 1993

Cavanaugh J. M., Walilko T., Chung J., King A. I., Abdominal Injury and Response in Side Impact, Proc. 40th Stapp Car Crash Conf., SAE Paper No: 962410, SAE , Warrendale, Pennsylvania, 1996

Cesari D., Bouquet R., Comparison of Hybrid III and human cadaver thorax deformations loaded by a thoracic belt, Proc. 38th Stapp Car Crash Conference, pp 65-76, SAE#942209, 1994

Chawla A., Mukherjee S., Mohan D., Jain S., Validation of the Cervical Spine Model in THUMS. 19th International Technical Conference on the Enhanced Safety of Vehicles, June 6-9, 2005. Paper No: 05-2005. Washington, D.C., USA, 2005

Deng Y-C, Li X and Ho H., Development of a Finite Element Thorax Model for Impact Injury Studies, SAE Paper No 1999-01-0715, Warrendale, Pennsylvania, 1999

DOT, Department of Transportation, National Highway Safety Administration, Federal Motor Vehicle Standards, Side Impact Protection, Rules 49, CFR Part 571 1990.

Eppinger R., Marcus J. H., Morgan R. M., Development of Dummy and Injury Index for NHTSA's Thoracic Side Impact Protection Research Program, SAE Paper No 840885, Government/Industry Meeting and Exposition, Washington, D.C., 1984

FAT ES-2 LS-Dyna User manual (2006), version 4.0, DYNAmore GmbH, 2006

Forbes P. A., Development of a Human Body Model for the Analysis of Side Impact Automotive Thoracic Trauma., Master Thesis, Waterloo, Ontario, Canada, 2005

Forbes P. A., Cronin, D. S., Deng, Y. C., Multi-scale human body model to predict side impact thoracic trauma, Int. J. Crashworthiness, Vol. 11, No. 3 pp 203-216. 2006

FTSS, FE Model Development, Technical Report, WorldSID 50th LS-Dyna Dummy Model, Version 1.0, Michigan, USA, 2005

Hovenga, P. E., Spit H. H., Uijldert M., Dalenport A. M. Improved Prediction of Hybrid-III Injury Values Using Advanced Multibody Techniques and Objective Rating. SAE Paper No 2005-01-1307, 2005

Koh S-W, Cavanaugh J. M., Zhu J., Injury and Response of the Shoulder in Lateral Sled Tests, Proc. 45th Stapp Car Crash Conf., SAE Paper No:2001-22-0005, SAE , Warrendale, Pennsylvania, 2001

Iwamoto M., Kazou M., Yang K., Development of a Finite Element Model of the Human Shoulder to Investigate the Mechanical Responses and Injuries in Side, JSME International Journal Series C, Vol. 44 No. 4, 2001

Iwamoto M., Recent Advances in THUMS: Development of the detailed head-neck and internal organs, and THUMS Family, LS-DYNA & JMAG User Conference 2003, Japan (in Japanese). 2003

Iwamoto M., Ankle Skeletal Injury Predictions Using Anisotropic Inelastic Constitutive Model of Cortical Bone Taking into Account Damage Evolution, Stapp Car Crash Journal, 49, 2005, pp133-156, 2005

Kent R., Crandall J., Bolton J., Prasad P., Nushotz G., Mertz H. The Influence of Superficial Soft Tissues and Restraint Condition on Thoracic Skeletal Injury Prediction. Stapp Car Crash Journal 45:183-203, 2001

Kent R., Lee S-H., Darvish K., Wang S., Poster C. S., Lange A. W., Brede C., Lange D., Structural and Material Changes in the Aging Thorax and Their Role in Crash Protection for Older Occupants, Stapp Car Crash Journal, Vol. 49, November 2005,

Lindquist M., Fatal Car Crash Configurations and Injury Panorama- with Special Emphasis on the Function of Restraint System, Ph.D. Thesis, Department of Surgical and Perioperative Science, Umeå University, Umeå 2007.

Oshita F., Kiyoshi M., Development of Finite Element Model of the Human Body. 7th International LS-Dyna Users Conference, Japan Automobile Research Institute and Toyota Central R&D Labs, Nagoya Japan, 2002

Peitjean A., Lebarbe M., Potier P., Torsseille S., Lassau J. Laboratory Reconstructions of Real World Frontal Crash Configurations Using the Hybrid III and THOR Dummies and PMHS. Paper 2002-22-0002, Stapp Car Crash Journal, 46:27-54, 2002

Rouhana S., Bedewi P., Kankanala S., Prasad P., Zwolinsi J., Meduvsky A., Rupp J., Jeffreys T., Schneider L. Biomechanics of 4-point Seat Belt Systems in Frontal Impacts. SAE Paper No, 2003-22-0017, 2003

Tortora, G., Principles of Anatomy and Physiology, New York: Harper Collins 8th Edition, ISBN 0-673-99354-X, 1996

Welsh R., Morris A., Hassan A., Injury Outcomes in Side Impacts Involving Modern Passenger Cars. Proc 20:th Int. Technical Conference on the Enhanced Safety of Vehicles, June 18-21 Lyon France, 2007

Yang K., Hu J., White N., King A., Chou C., Prasad P. Development of Numerical Models for Injury Biomechanics Research: A Review of 50 Years of Publications in the Stapp Car Crash Conference, Paper 2006-22-0017, Stapp Car Crash Journal, 50:429-490, 2006.

APPENDIX A: BOLTE PENDULUM RESULT PLOTS
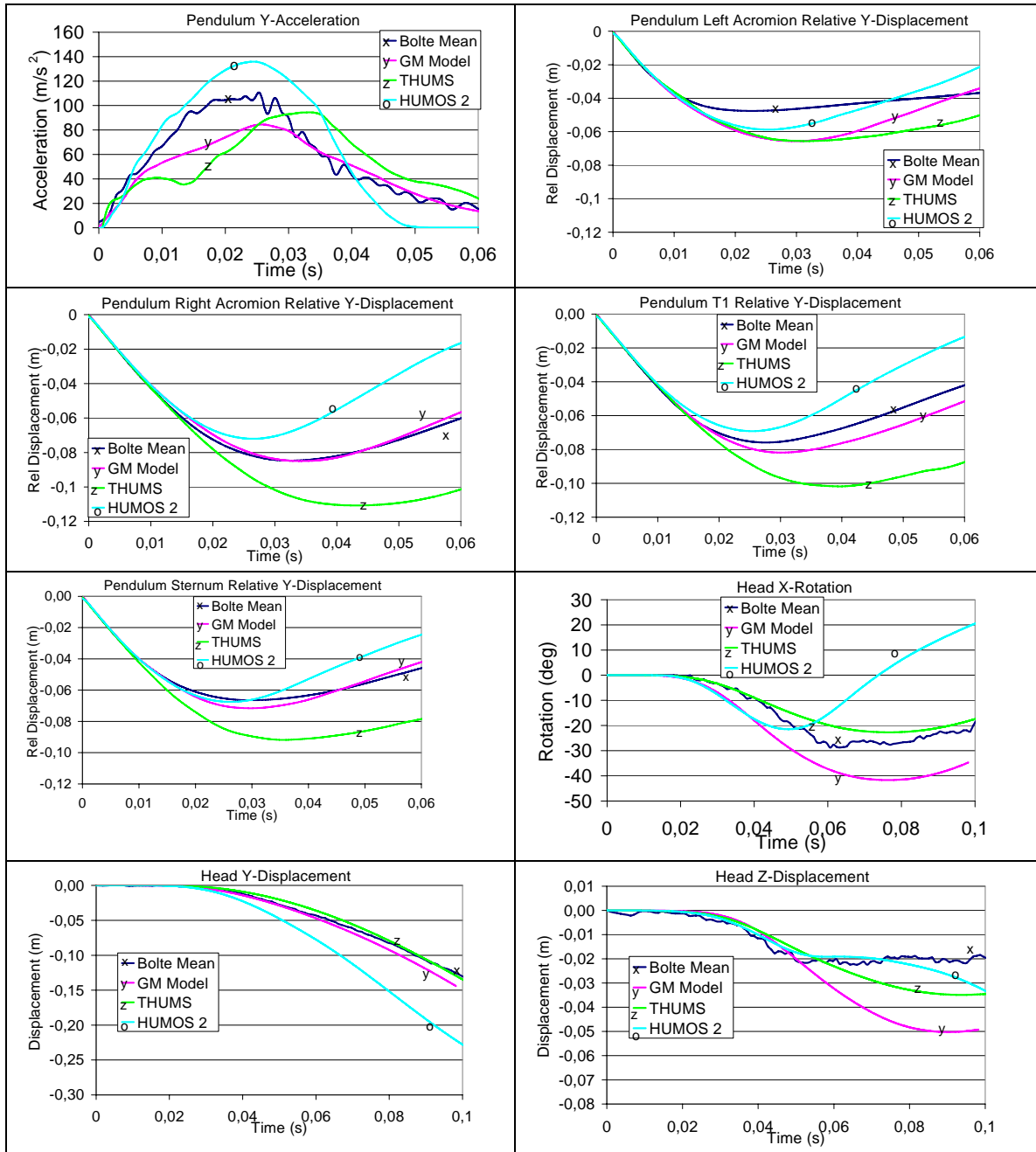
APPENDIX B: WAYNE STATE SLED RESULT PLOTS